

# Supplementary Material of Single-Image Super-Resolution: A Benchmark

Chih-Yuan Yang<sup>1</sup>, Chao Ma<sup>12</sup>, and Ming-Hsuan Yang<sup>1</sup>

<sup>1</sup>University of California at Merced

<sup>2</sup>Shanghai Jiao Tong University

{cyang35, cma26, mhyang}@ucmerced.edu

## 1 Test Image Sets

The test images sets used in the benchmark evaluations are the BSD200 and LIVE1 datasets, which contain 200 and 29 images respectively. Fig. 1 and Fig. 2 show some examples of the two datasets which cover a wide range of image contents.

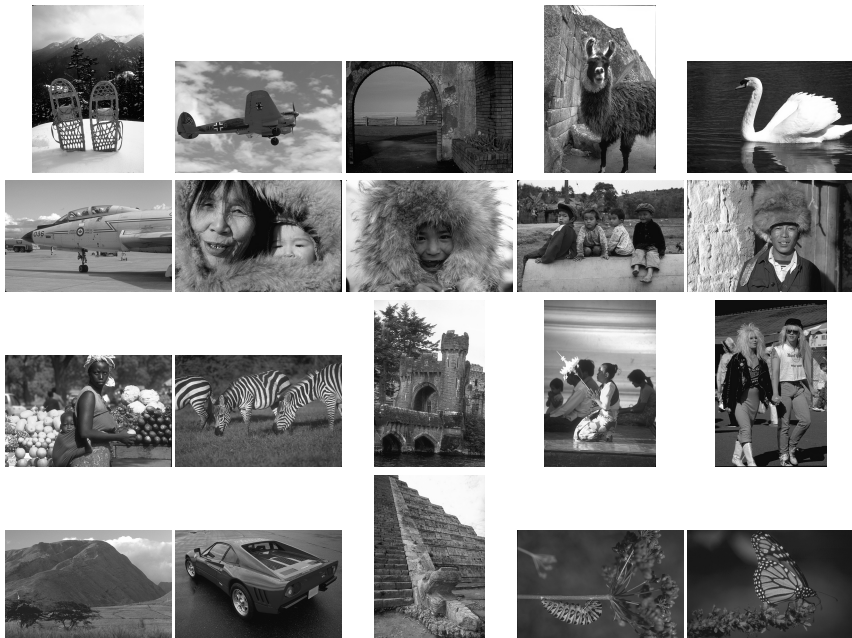


**Fig. 1.** The first 20 images of the BSD200 dataset.

As mentioned on line 184 of the manuscript, Fig. 3 shows the 10 images used in the human subject studies and the ranks of the PSNR values in the BSD200 dataset. Higher ranked images contain more high-frequency details. As the ranks



**Fig. 2.** The first 20 images of the LIVE1 dataset.

are evenly distributed, they form a representative subset of the BSD200 dataset that can be used to compute the correlation coefficients between perceptual scores and metric indices.

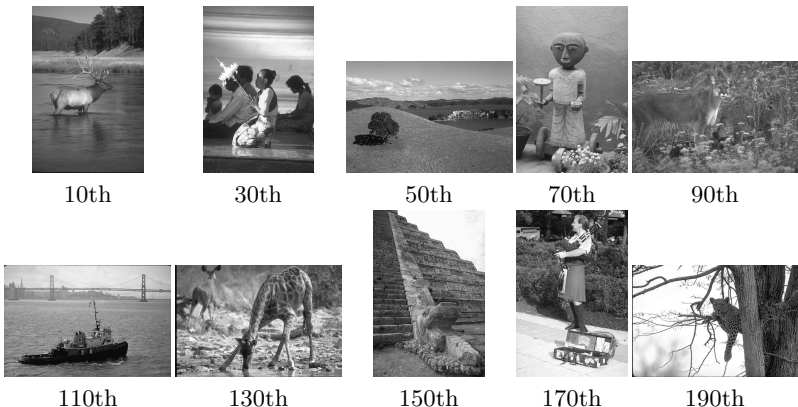


**Fig. 3.** The 10 images used in human subject studies and their ranks of PSNR values.

## 2 Performance Evaluation

As mentioned on line 205 of the manuscript, Fig. 4 and Fig. 5 show the complete evaluations including the SLJT, FF, and DZSW methods. As mentioned on line 175 of the manuscript, the released codes of the SSXS, KK, and FF methods only support scaling factors 2, 3, and 4. The released code of the DZSW method does not converge for kernel width of 0.4 and 0.6.

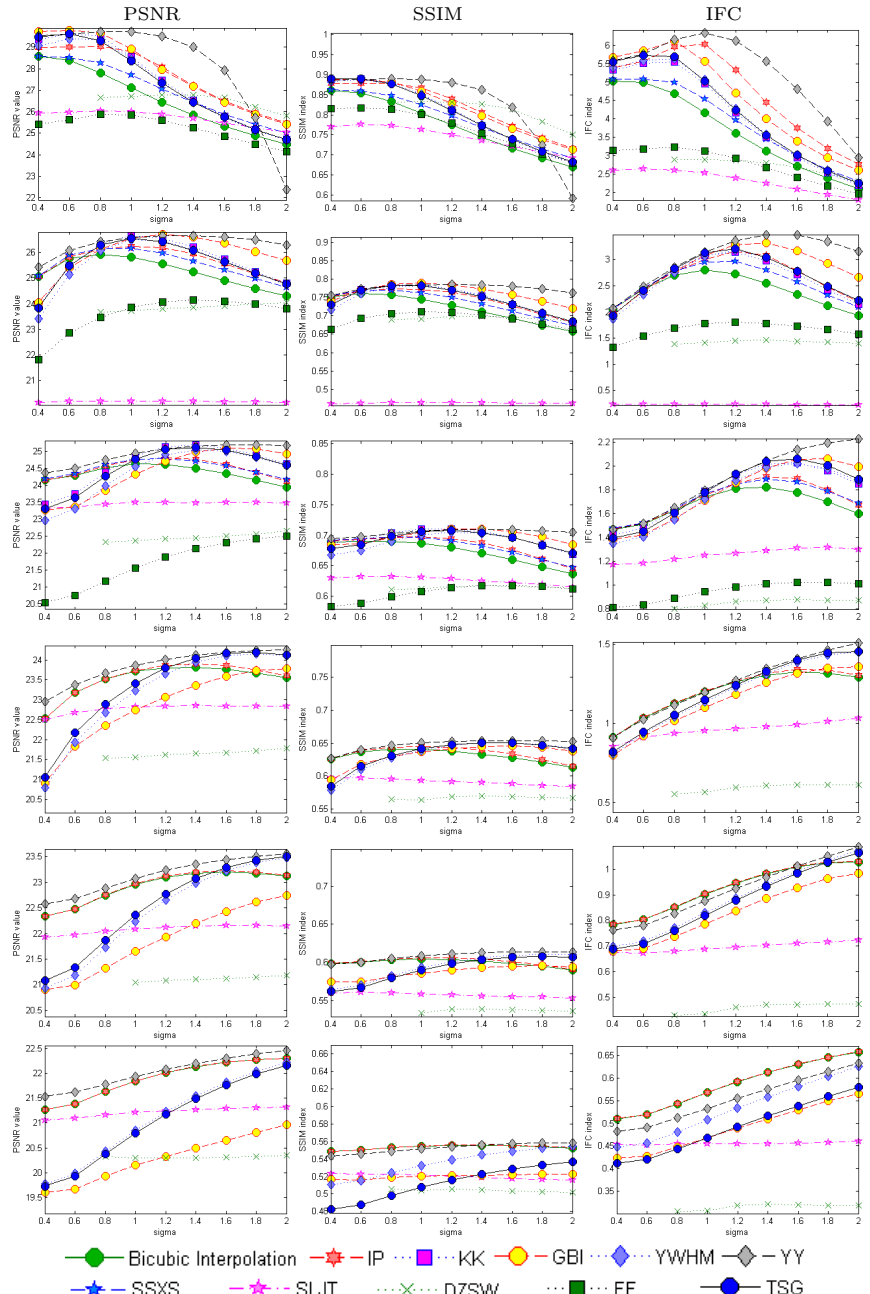


**Fig. 4.** Performance evaluation. Eleven SISR methods are evaluated using the BSD200 dataset and three metrics (PSNR, SSIM, and IFC) under six scaling factors and nine kernel width values. From top to bottom, each row shows results of a scaling factor of 2, 3, 4, 5, 6, and 8. The plots show mean values for all SR images of the dataset.

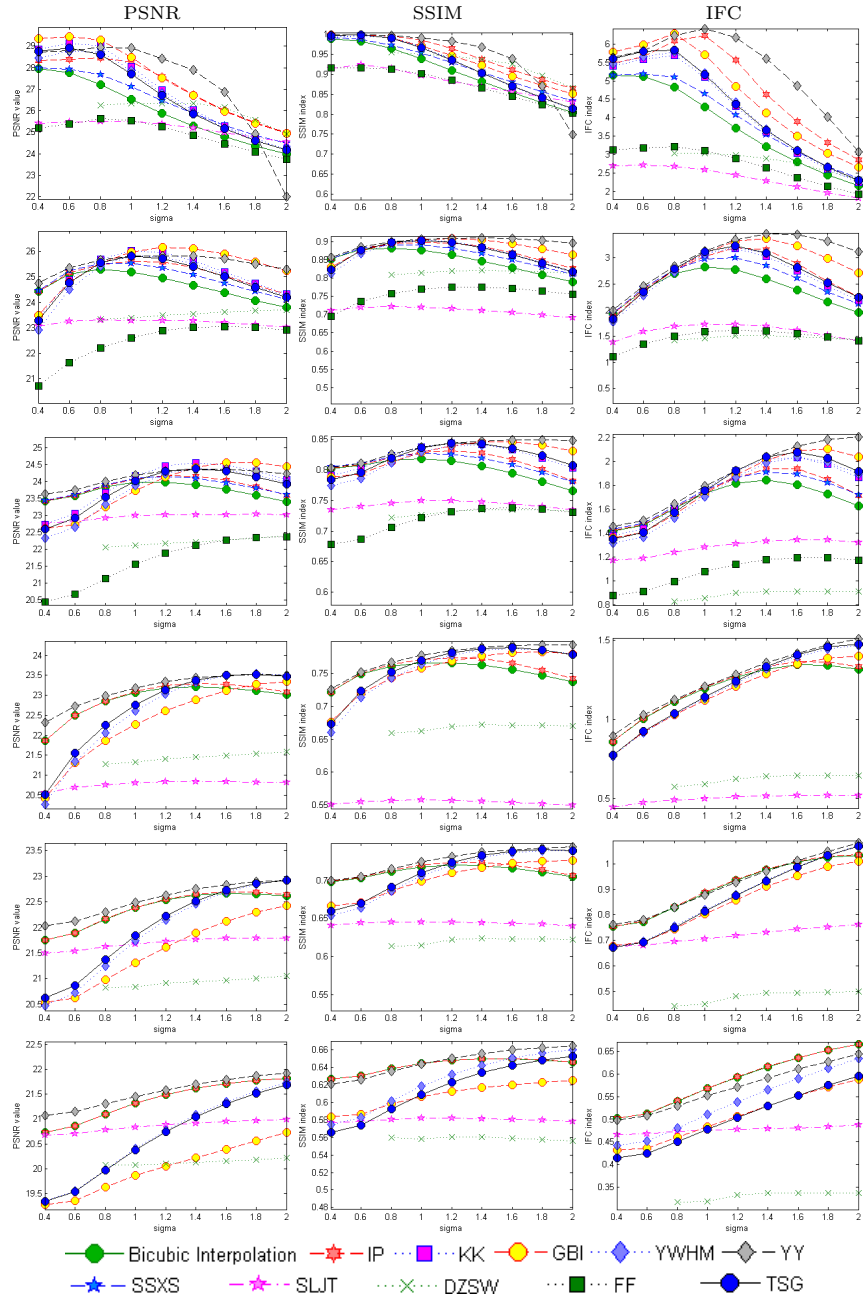


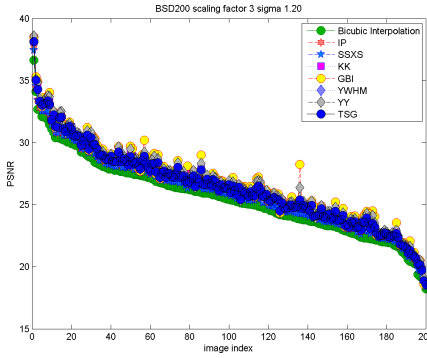
**Fig. 5.** Performance evaluation. Eleven SISR methods are evaluated using the LIVE1 dataset and three metrics (PSNR, SSIM, and IFC) under six scaling factors and nine kernel width values. From top to bottom, each row shows results of a scaling factor of 2, 3, 4, 5, 6, and 8. The plots show mean values for all SR images of the dataset.

### 3 More Correlation Coefficients

As mentioned on line 316 of the manuscript, the performance of a super-resolution image is primarily determined by the image content. Fig. 6-10 show the supplementary data to Fig. 2 of the manuscript for other scaling factors (3, 4, 5, 6, 8). The images of the highest and lowest PSNR values are almost all the same across all the scaling factors. Table 1-6 show the Pearson product-moment correlation coefficients of PSNR values of images generated by various settings and methods. Each coefficient is computed between two sets of PSNR values. The first set is fixed and generated by the bicubic interpolation method under a setting of scaling factor of 2 and blur kernel width of 1.2. The second set is determined by a scaling factor, the SISR method, and  $\sigma$  values of each table. These high correlation coefficients show that the performance is unlikely affected by the scaling factors, SISR methods, and blur kernel width.

**Table 1.** The correlation coefficients of the scaling factor of 2.

SISR method	$\sigma$ (Gaussian kernel width)								
	0.4	0.6	0.8	1.0	1.2	1.4	1.6	1.8	2.0
Bicubic Interpolation	0.9915	0.9934	0.9969	0.9992	1.0000	0.9993	0.9975	0.9949	0.9917
IP	0.9882	0.9884	0.9874	0.9860	0.9888	0.9943	0.9978	0.9992	0.9992
GBI	0.9573	0.9961	0.9968	0.9975	0.9889	0.9950	0.9990	0.9982	0.9970
KK	0.9680	0.9683	0.9779	0.9907	0.9976	0.9997	0.9989	0.9966	0.9934
YWHM	0.9756	0.9754	0.9826	0.9932	0.9987	0.9999	0.9989	0.9961	0.9928
YY	0.9735	0.9728	0.9722	0.9727	0.9726	0.9727	0.9691	0.9458	0.8574
SSXS	0.9855	0.9871	0.9911	0.9952	0.9982	0.9996	0.9997	0.9986	0.9966
TSG	0.9709	0.9723	0.9818	0.9926	0.9983	0.9999	0.9989	0.9965	0.9932



(a) ranked values

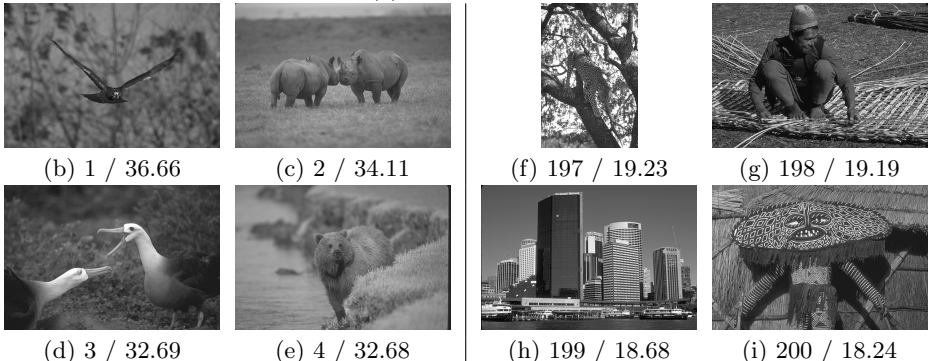
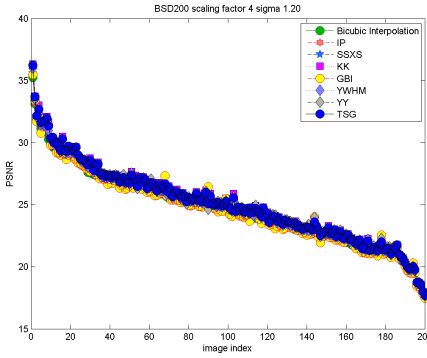


**Fig. 6.** Results of the scaling factor of 3 and  $\sigma$  of 1.2. (a) PSNR values. (b)-(e) The four images of the highest PSNR values. (f)-(i) The four images of the lowest PSNR values.

**Table 2.** The correlation coefficients of the scaling factor of 3.

SISR method	$\sigma$ (Gaussian kernel width)									
	0.4	0.6	0.8	1.0	1.2	1.4	1.6	1.8	2.0	
Bicubic Interpolation	0.9972	0.9987	0.9994	0.9995	0.9990	0.9977	0.9958	0.9931	0.9901	
IP	0.9972	0.9986	0.9990	0.9991	0.9990	0.9989	0.9987	0.9983	0.9970	
GBI	0.9952	0.9936	0.9915	0.9900	0.9895	0.9902	0.9917	0.9930	0.9938	
KK	0.9947	0.9943	0.9937	0.9944	0.9964	0.9982	0.9986	0.9973	0.9947	
YWBM	0.9974	0.9976	0.9969	0.9969	0.9981	0.9992	0.9990	0.9971	0.9941	
YY	0.9971	0.9964	0.9957	0.9952	0.9945	0.9942	0.9935	0.9922	0.9904	
SSXS	0.9967	0.9982	0.9988	0.9992	0.9994	0.9993	0.9983	0.9966	0.9942	
TSG	0.9956	0.9953	0.9948	0.9955	0.9974	0.9988	0.9988	0.9973	0.9945	



(a) ranked values

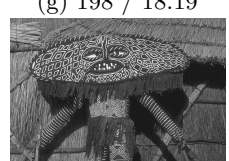


**Fig. 7.** Results of the scaling factor of 4 and  $\sigma$  of 1.2. (a) PSNR values. (b)-(e) The four images of the highest PSNR values. (f)-(i) The four images of the lowest PSNR values.

**Table 3.** The correlation coefficients of the scaling factor of 4.

SISR method	$\sigma$ (Gaussian kernel width)								
	0.4	0.6	0.8	1.0	1.2	1.4	1.6	1.8	2.0
Bicubic Interpolation	0.9965	0.9963	0.9959	0.9954	0.9945	0.9932	0.9914	0.9890	0.9863
IP	0.9965	0.9963	0.9961	0.9961	0.9962	0.9961	0.9955	0.9938	0.9909
GBI	0.9958	0.9950	0.9935	0.9932	0.9934	0.9936	0.9938	0.9940	0.9935
KK	0.9958	0.9958	0.9960	0.9964	0.9967	0.9968	0.9966	0.9957	0.9939
YWBM	0.9957	0.9957	0.9960	0.9967	0.9972	0.9974	0.9970	0.9958	0.9937
YY	0.9946	0.9948	0.9953	0.9956	0.9957	0.9959	0.9961	0.9956	0.9953
SSXS	0.9967	0.9965	0.9963	0.9961	0.9958	0.9950	0.9937	0.9919	0.9895
TSG	0.9961	0.9960	0.9960	0.9964	0.9967	0.9968	0.9965	0.9955	0.9936

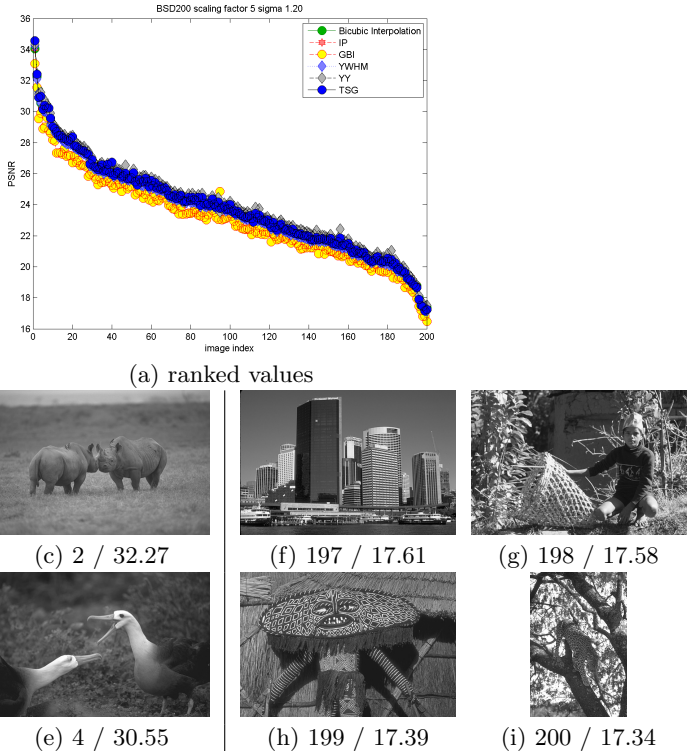
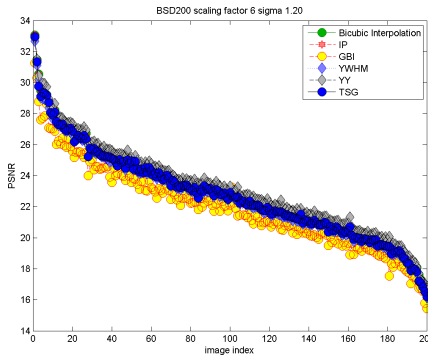


**Fig. 8.** Results of the scaling factor of 5 and  $\sigma$  of 1.2. (a) PSNR values. (b)-(e) The four images of the highest PSNR values. (f)-(i) The four images of the lowest PSNR values.

**Table 4.** The correlation coefficients of the scaling factor of 5.

SISR method	$\sigma$ (Gaussian kernel width)								
	0.4	0.6	0.8	1.0	1.2	1.4	1.6	1.8	2.0
Bicubic Interpolation	0.9923	0.9890	0.9878	0.9873	0.9867	0.9859	0.9846	0.9828	0.9807
IP	0.9923	0.9890	0.9879	0.9878	0.9879	0.9878	0.9871	0.9855	0.9825
GBI	0.9915	0.9857	0.9814	0.9802	0.9799	0.9803	0.9835	0.9843	0.9840
KK	N.A.	N.A.	N.A.	N.A.	N.A.	N.A.	N.A.	N.A.	N.A.
YWHM	0.9920	0.9866	0.9849	0.9859	0.9877	0.9892	0.9901	0.9902	0.9894
YY	0.9851	0.9858	0.9867	0.9878	0.9887	0.9894	0.9897	0.9901	0.9903
SSXS	N.A.	N.A.	N.A.	N.A.	N.A.	N.A.	N.A.	N.A.	N.A.
TSG	0.9926	0.9878	0.9864	0.9871	0.9885	0.9896	0.9901	0.9900	0.9891



(a) ranked values

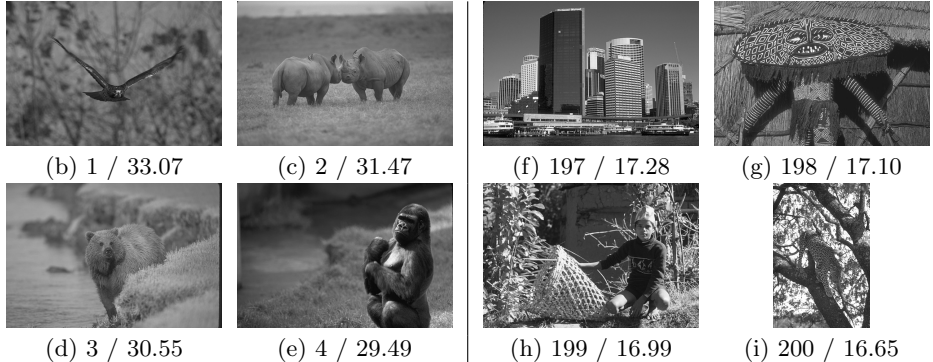


**Fig. 9.** Results of the scaling factor of 6 and  $\sigma$  of 1.2. (a) PSNR values. (b)-(e) The four images of the highest PSNR values. (f)-(i) The four images of the lowest PSNR values.

**Table 5.** The correlation coefficients of the scaling factor of 6.

SISR method	$\sigma$ (Gaussian kernel width)								
	0.4	0.6	0.8	1.0	1.2	1.4	1.6	1.8	2.0
Bicubic Interpolation	0.9785	0.9778	0.9769	0.9766	0.9765	0.9762	0.9756	0.9745	0.9731
IP	0.9785	0.9778	0.9770	0.9768	0.9770	0.9771	0.9768	0.9756	0.9737
GBI	0.9706	0.9676	0.9634	0.9605	0.9592	0.9594	0.9630	0.9657	0.9675
KK	N.A.	N.A.	N.A.	N.A.	N.A.	N.A.	N.A.	N.A.	N.A.
YWHM	0.9732	0.9717	0.9701	0.9707	0.9729	0.9757	0.9781	0.9798	0.9806
YY	0.9728	0.9733	0.9748	0.9761	0.9776	0.9788	0.9797	0.9806	0.9812
SSXS	N.A.	N.A.	N.A.	N.A.	N.A.	N.A.	N.A.	N.A.	N.A.
TSG	0.9740	0.9727	0.9711	0.9716	0.9737	0.9761	0.9782	0.9796	0.9802

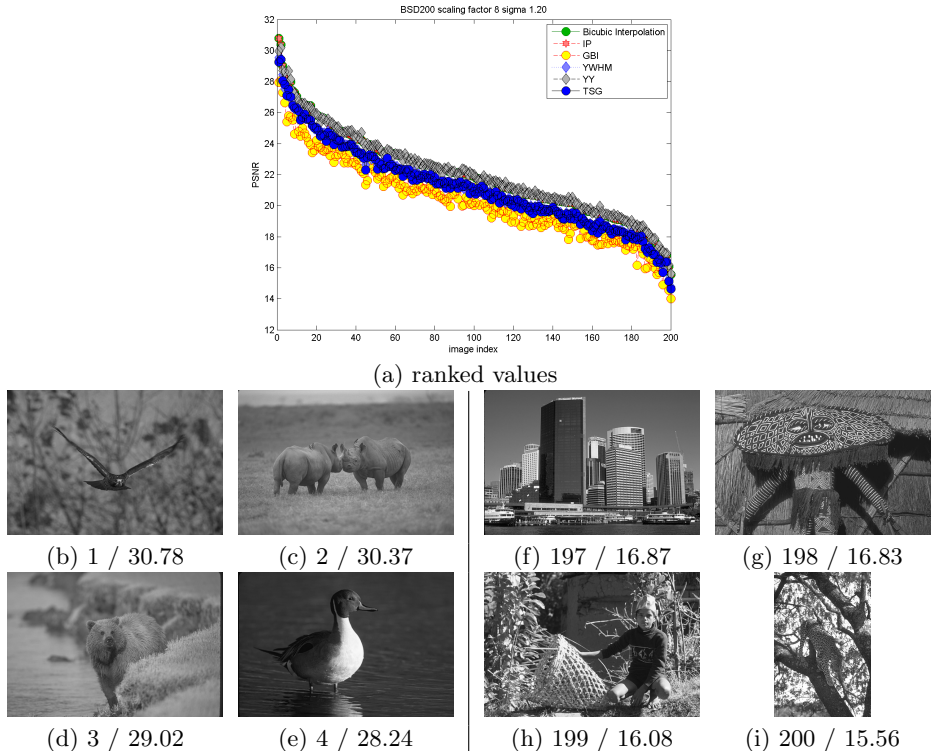


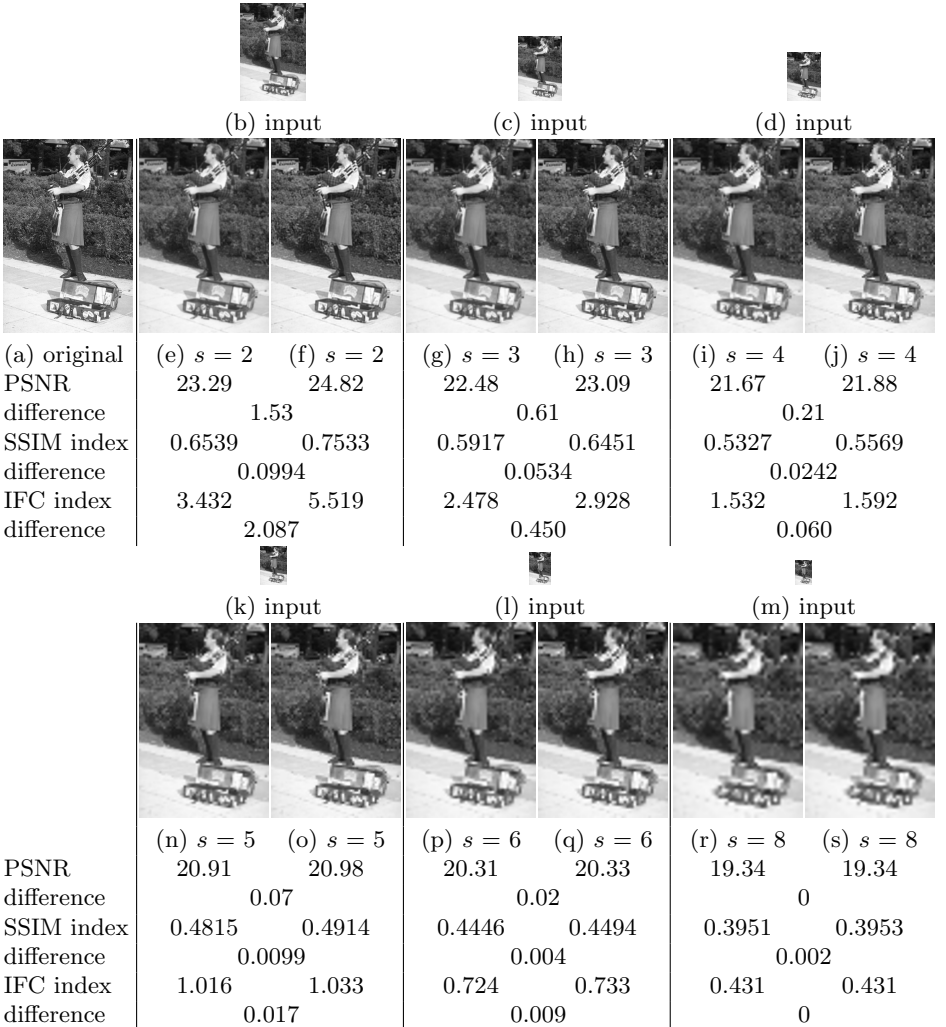
**Fig. 10.** Results of the scaling factor of 8 and  $\sigma$  of 1.2. (a) PSNR values. (b)-(e) The four images of the highest PSNR values. (f)-(i) The four images of the lowest PSNR values.

**Table 6.** The correlation coefficients of the scaling factor of 8.

SISR method	$\sigma$ (Gaussian kernel width)									
	0.4	0.6	0.8	1.0	1.2	1.4	1.6	1.8	2.0	
Bicubic Interpolation	0.9564	0.9552	0.9535	0.9531	0.9535	0.9542	0.9547	0.9550	0.9549	
IP	0.9564	0.9552	0.9535	0.9531	0.9535	0.9542	0.9548	0.9551	0.9550	
GBI	0.9417	0.9367	0.9293	0.9245	0.9199	0.9172	0.9161	0.9151	0.9182	
KK	N.A.	N.A.	N.A.	N.A.	N.A.	N.A.	N.A.	N.A.	N.A.	
YWHM	0.9490	0.9463	0.9421	0.9405	0.9416	0.9445	0.9480	0.9516	0.9549	
YY	0.9444	0.9455	0.9474	0.9496	0.9520	0.9540	0.9558	0.9574	0.9586	
SSXS	N.A.	N.A.	N.A.	N.A.	N.A.	N.A.	N.A.	N.A.	N.A.	
TSG	0.9464	0.9436	0.9391	0.9375	0.9385	0.9413	0.9449	0.9485	0.9518	

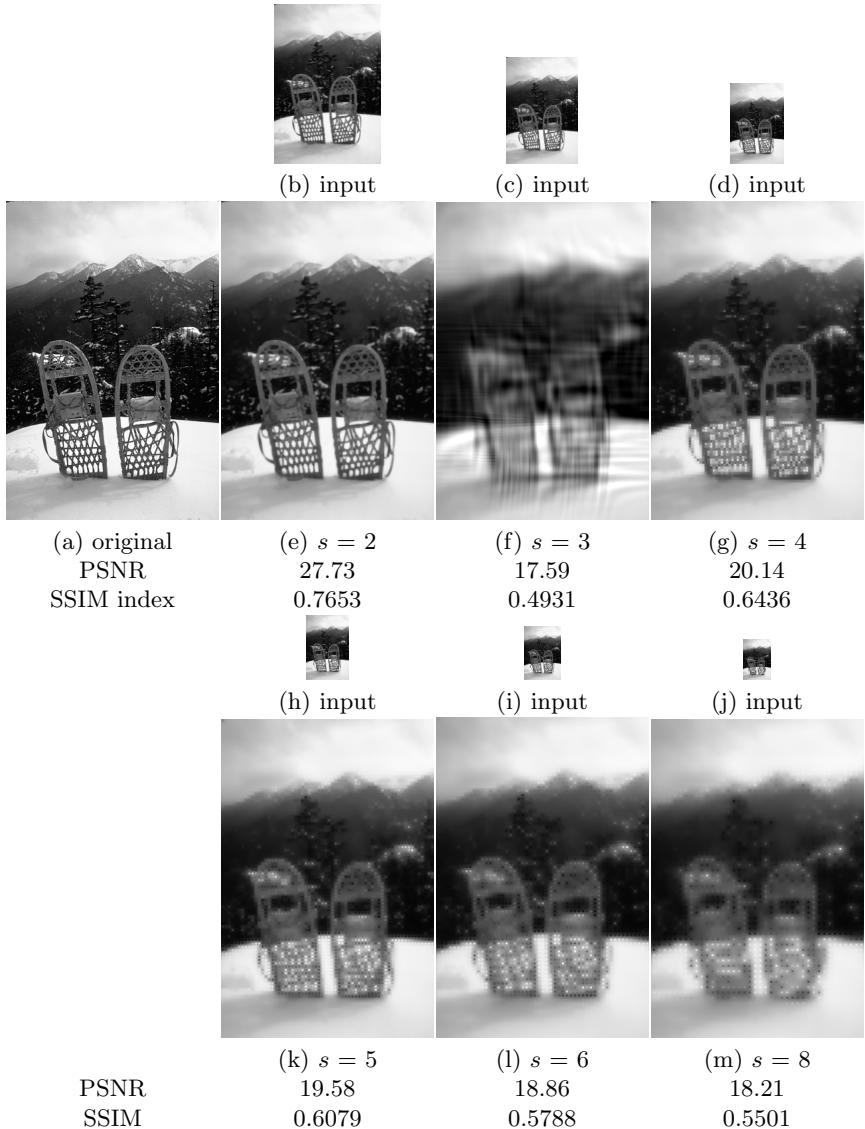
## 4 More Experimental Results

Fig. 11 shows images generated by the bicubic interpolation and IP methods. As mentioned on line 428 to 430 of the manuscript, images generated by the IP method have better contrast. The images generated by the IP method with larger scaling factors have similar metric indices as the ones generated by the bicubic interpolation (e.g,  $s \geq 5$ ). That is, the IP method performs better than bicubic interpolation when the scaling factor  $s$  is less than or equal to 4.



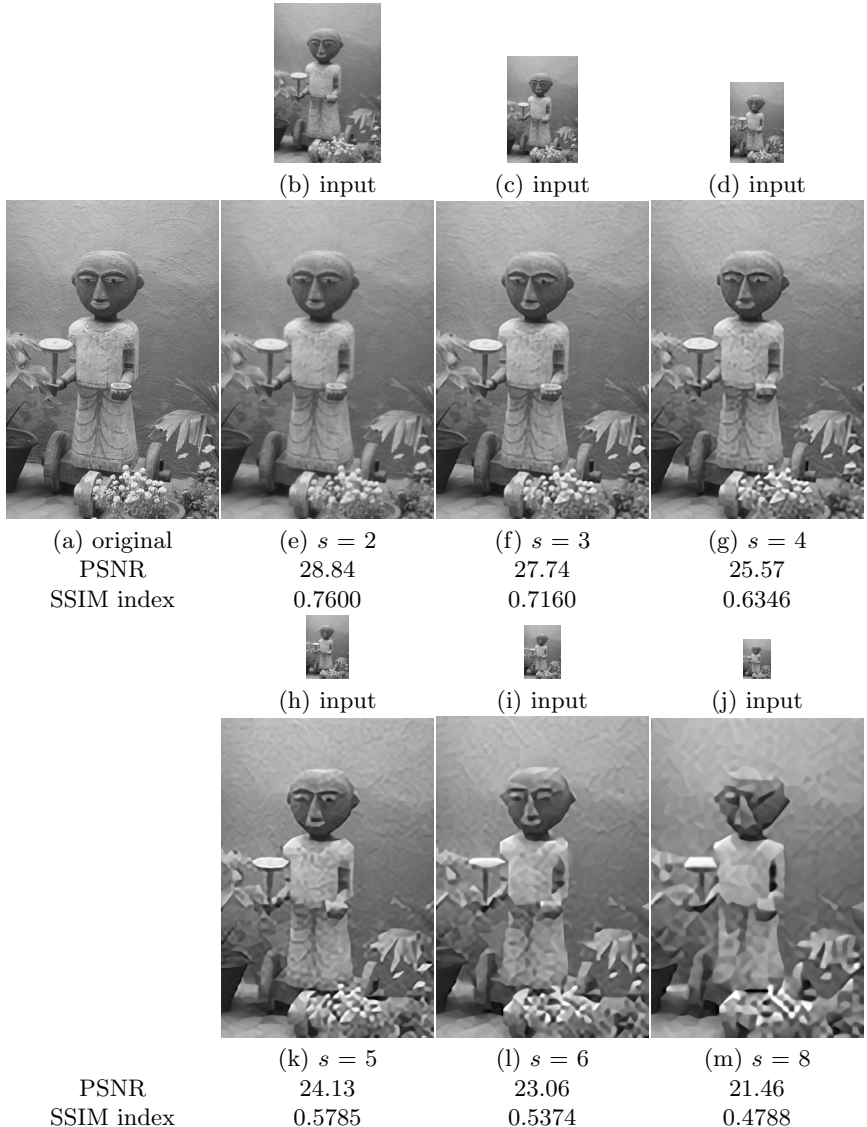
**Fig. 11.** Comparisons of the bicubic interpolation and IP methods. (e)(g)(i)(n)(p)(r) Images generated by the bicubic interpolation method. (f)(h)(j)(o)(q)(s) Images generated by the IP method. Super-resolution images are best viewed on a high-resolution display with an adequate zoom level where each image is shown with at least  $321 \times 481$  pixels (full-resolution).

Fig. 12 shows images generated by the released code of the SLJT method. The release code does not work correctly for the scaling factor of 3.



**Fig. 12.** Images generated by the SLJT method using blur kernel width of 1.2 and different scaling factors ( $s$ ). The generated image of the scaling factor of 3 contains over-smoothed edges and ghost artifacts. Super-resolution images are best viewed on a high-resolution display with an adequate zoom level where each image is shown with at least  $321 \times 481$  pixels (full resolution).

Fig. 13 shows images generated by the GBI method. As mentioned on line 497 of the manuscript, for small scaling factors such as 2, 3, and 4, the edges are adequately sharp and the textures are not blocky. For large scaling factors greater than 4, the edges are over-sharpened and the textures contain obvious blocky artifacts.



**Fig. 13.** Images generated by the GBI method using blur kernel width of 1.2 and different scaling factors  $s$ . Super-resolution images are best viewed on a high-resolution display with an adequate zoom level where each image is shown with at least  $321 \times 481$  pixels (full resolution).

Fig. 14 to Fig. 19 compare images generated by the 11 evaluated methods using images of the 70th and 170th ranks (see Fig. 3). Some perceptual scores are not available as the images are not used in the human subject studies.

					
(a) input		(c) Bicubic Int.	(d) IP	(e) SLJT	(f) GBI
PSNR	27.55	28.96	27.04	28.84	
SSIM index	0.7089	0.7735	0.6757	0.7600	
perceptual score	N.A.	5.65	N.A.	6.05	
IFC index	3.637	5.257	2.320	4.725	
					
(b) original		(g) KK	(h) YWHM	(i) DZSW	(j) YY
PSNR	28.43	28.39	27.78	<b>30.05</b>	
SSIM index	0.7442	0.7509	0.7711	<b>0.7958</b>	
perceptual score	4.85	4.90	<b>7.80</b>	6.85	
IFC index	4.181	4.394	2.939	<b>5.718</b>	
					
(k) SSXS		(l) TSG	(m) FF		
PSNR	28.10	28.36	26.52		
SSIM index	0.7317	0.7470	0.7205		
perceptual score	N.A.	N.A.	N.A.		
IFC index	3.955	4.328	3.039		

**Fig. 14.** Comparison of super-resolution images of the scaling factor of 2 and  $\sigma$  of 1.2. Images are best viewed on a high-resolution display with an adequate zoom level where each super-resolution image is shown with at least  $320 \times 480$  pixels (full-resolution).

(a) input PSNR SSIM index perceptual score IFC index	(c) Bicubic Int. 26.74 0.6640 3.08 2.645	(d) IP 27.36 0.6996 3.85 3.050	(e) SLJT 21.30 0.4435 N.A. 0.189	(f) GBI <b>27.74</b> <b>0.7160</b> 4.31 3.173	
(b) original PSNR SSIM index perceptual score IFC index	(g) KK 27.70 0.7058 4.38 3.074	(h) YWHM 27.55 0.7063 4.77 3.075	(i) DZSW 24.88 0.6352 N.A. 1.379	(j) YY 27.67 0.7111 <b>4.85</b> <b>3.176</b>	
PSNR SSIM index perceptual score IFC index	(k) SSXS 27.15 0.6838 N.A. 2.869	(l) TSG 27.56 0.7044 N.A. 3.106	(m) FF 24.88 0.6492 N.A. 1.745		

**Fig. 15.** Comparison of super-resolution images of the scaling factor of 3 and  $\sigma$  of 1.2. Images are best viewed on a high-resolution display with an adequate zoom level where each super-resolution image is shown with at least  $321 \times 480$  pixels (full-resolution).

(a) input PSNR SSIM index perceptual score IFC index	(c) Bicubic Int. 25.86 0.6183 1.50 1.638	(d) IP 26.08 0.6343 2.00 1.694	(e) SLJT 24.72 0.5713 N.A. 1.178	(f) GBI 25.57 0.6346 1.88 1.715	
(b) original PSNR SSIM index perceptual score IFC index	(g) KK <b>26.38</b> <b>0.6481</b> <b>2.50</b> <b>1.776</b>	(h) YWHM 26.14 0.6435 1.63 1.705	(i) DZSW 23.44 0.5589 N.A. 0.755	(j) YY 26.25 0.6429 2.00 1.754	
PSNR SSIM index perceptual score IFC index	(k) SSXS 26.04 0.6285 N.A. 1.690	(l) TSG 26.30 0.6465 N.A. 1.762	(m) FF 21.97 0.5417 N.A. 0.861		

**Fig. 16.** Comparison of super-resolution images of the scaling factor of 4 and  $\sigma$  of 1.2. Images are best viewed on a high-resolution display with an adequate zoom level where each super-resolution image is shown with at least  $320 \times 480$  pixels (full-resolution).

					
(a) input		(c) Bicubic Int.	(d) IP	(e) SLJT	(f) GBI
PSNR		23.29	24.82	22.84	24.52
SSIM index		0.6539	0.7533	0.6245	0.7256
perceptual score		N.A.	5.16	N.A.	5.00
IFC index		3.432	5.519	2.284	4.641
					
(b) original		(g) KK	(h) YWHM	(i) DZSW	(j) YY
PSNR		24.17	24.13	23.65	<b>26.09</b>
SSIM index		0.7081	0.7107	0.7497	<b>0.8179</b>
perceptual score		4.42	4.53	<b>7.58</b>	6.74
IFC index		4.13	4.216	2.786	<b>6.464</b>
					
PSNR		(k) SSXS	(l) TSG	(m) FF	
SSIM index		23.81	24.08	22.89	
perceptual score		0.6860	0.7049	0.6693	
IFC index		N.A.	N.A.	N.A.	
		3.819	4.143	2.887	

**Fig. 17.** Comparison of super-resolution images of the scaling factor of 2 and  $\sigma$  of 1.2. Images are best viewed on a high-resolution display with an adequate zoom level where each super-resolution image is shown with at least  $320 \times 480$  pixels (full-resolution).

					
(a) input		(c) Bicubic Int.	(d) IP	(e) SLJT	(f) GBI
PSNR		22.48	23.09	17.45	<b>23.40</b>
SSIM index		0.5917	0.6451	0.3000	0.6687
perceptual score		2.33	3.08	N.A.	2.58
IFC index		2.478	2.928	0.180	3.063
					
(b) ground truth		(g) KK	(h) YWHM	(i) DZSW	(j) YY
PSNR		23.31	23.25	20.98	<b>23.40</b>
SSIM index		0.6485	0.6501	0.5679	<b>0.6689</b>
perceptual score		4.17	3.75	N.A.	<b>4.25</b>
IFC index		2.916	2.934	1.303	<b>3.076</b>
					
PSNR		(k) SSXS	(l) TSG	(m) FF	
SSIM index		0.6180	0.6460	0.5766	
perceptual score		N.A.	N.A.	N.A.	
IFC index		2.709	2.949	1.642	

**Fig. 18.** Comparison of super-resolution images of the scaling factor of 3 and  $\sigma$  of 1.2. Images are best viewed on a high-resolution display with an adequate zoom level where each super-resolution image is shown with at least  $321 \times 480$  pixels (full-resolution).

					
(a) input		(c) Bicubic Int.	(d) IP	(e) SLJT	(f) GBI
PSNR	21.67	21.88	20.75	21.47	
SSIM index	0.5327	0.5569	0.4775	0.5670	
perceptual score	1.13	1.50	N.A.	1.13	
IFC index	1.532	1.592	1.158	1.641	
					
(b) ground truth		(g) KK	(h) YWHM	(i) DZSW	(j) YY
PSNR	<b>22.08</b>	21.90	19.84	22.06	
SSIM index	0.5712	0.5683	0.4742	<b>0.5724</b>	
perceptual score	1.38	1.50	N.A.	<b>1.6</b>	
IFC index	1.637	1.594	0.752	<b>1.674</b>	
					
PSNR	(k) SSXS	(l) TSG	(m) FF		
SSIM index	21.83	22.03	19.04		
perceptual score	0.5466	0.5702	0.4621		
IFC index	N.A.	N.A.	N.A.		

**Fig. 19.** Comparison of super-resolution images of the scaling factor of 4 and  $\sigma$  of 1.2. Images are best viewed on a high-resolution display with an adequate zoom level where each super-resolution image is shown with at least  $320 \times 480$  pixels (full-resolution).